
Revisit Weakly-Supervised Audio-Visual Video Parsing from the Language Perspective

Yingying Fan, Yu Wu, Yutian Lin, Bo Du

School of Computer Science, Hubei Luojia Laboratory, Wuhan University
 {fanyingying_cs, wuyucs, yutian.lin, dubo}@whu.edu.cn

Abstract

We focus on the weakly-supervised audio-visual video parsing task (AVVP), which aims to identify and locate all the events in audio and visual modalities. Previous works only concentrate on video-level overall label denoising across modalities, but overlook the segment-level label noise, where adjacent video segments (*i.e.*, 1-second video clips) may contain different events. However, recognizing events in the segment is challenging because its label could be any combination of events that occur in the video. To address this issue, we consider tackling AVVP from the language perspective, since language could freely describe how various events appear in each segment beyond fixed labels. Specifically, we design language prompts to describe all cases of event appearance for each video. Then, the similarity between language prompts and segments is calculated, where the event of the most similar prompt is regarded as the segment-level label. In addition, to deal with the mislabeled segments, we propose to perform dynamic re-weighting on the unreliable segments to adjust their labels. Experiments show that our simple yet effective approach outperforms state-of-the-art methods by a large margin.

1 Introduction

Classic audio-visual tasks such as audio-visual event localization and audio-visual representation learning have been well explored in previous works [1, 2, 3] and have achieved promising performance. However, most existing research studies on these tasks assume that audio and visual are correlated and temporally aligned, which is not always the case. For example, a person can hear a dog barking but not see it in the video. To this end, we focus on the more general audio-visual video parsing (AVVP) task, which aims to recognize all events in each modality and localize their temporal boundaries.

Since the full annotation process is time-consuming and expensive, Tian *et al.* [4] address AVVP in a weakly-supervised manner, which only requires video-level labels, without specifying the modality and temporal boundaries. They develop a hybrid attention network to leverage unimodal and cross-modal information and propose a simple Multimodal Multiple Instance Learning (MMIL) framework to aggregate segment-level predictions into video-level ones. However, weakly-supervised labels cannot determine which modality the event comes from. Wu *et al.* [5] then introduce a video-level label refinement method and adopt contrastive learning for audio and visual temporal alignment. Furthermore, Chen *et al.* [6] propose another label denoising method based on alleviating modality-specific noise through cross-modal loss patterns for both modalities.

However, previous works [5, 6] only considered the noisy label at the overall video instance level, while ignoring the **segment-level label noise**. Segment-level label noise indicates the fact that *not every segment of a video contains all the events of the video*. For example, a person may be *speaking* in the video for a few seconds, and then he disappears in the following seconds. Therefore, it is inappropriate to consider *speech* as a supervised signal for all segments, where *speech* can be regarded

as a noisy label for some segments of this video. It could harm the network in event classification on segments when training with such segment-level noisy labels.

The challenge of learning reliable segment-level labels comes from that the label of each segment is not predefined, but could be any combination of events that occur in the video, *e.g.*, a segment may contain both speech and music events or none of them. To address this flexible label assignment challenge, we propose to leverage a third modality, the language, which enables better scene understanding beyond the labels. Language can describe what is happening in the scene, and who is involved, and identify segments not covered by the existing labels. Therefore, we propose to address AVVP from the language perspective, where natural language descriptions are served as a bridge connecting video and flexible weak labels.

In this paper, we propose a **Language guided Segment-level Label Denoising (LSDL)** strategy. We leverage the generalization capability of language to construct prompts that indicate all cases of event appearance for a segment. To connect vision and language, we introduce a vision-language pre-trained model, CLIP [7], into our work. Specifically, CLIP is used to extract the visual features for all segments, and the similarity between the segment and all prompts is calculated for label denoising. In addition, to further mitigate the effect of noisy segment labels, we perform a dynamic re-weighting strategy on the segments that may be mislabeled. Specifically, we calculate the similarity between the language description of each event and all the segments across the dataset. We do this for both the segments with or without the event label (*i.e.*, potentially positive and negative clips) separately to compare their similarity distribution. If a segment’s similarity falls within the overlap of the positive and negative groups, we consider it an unreliable segment and adjust its label dynamically according to its similarity to the event.

Note that, we do not assign segment-level labels for the audio track because audio is more continuous on segments and the existing audio-language model [8, 9] can only classify on the video level. However, since there is a natural connection between visual and audio, the audio branch could infer the event information from the reliable visual branch. As a result, our approach significantly outperforms the state-of-the-art on all visual metrics. The main contributions of our work are summarized as follows:

- We introduce the language modality to the AVVP task and construct language prompts that indicate all cases of event appearance for a segment, where the prompt with the highest similarity is regarded as segment-level label noise.
- We propose a simple yet effective Language-guided Segment-level Label Denoising (LSDL) mechanism based on CLIP to align the modality of visual and language for segment-level label denoising. In addition, we mine the segments with unreliable labels and learn from them with dynamic weight.
- Experiments show our method achieves comparable performance with the state-of-the-art methods. Especially, we improve visual metric significantly from 63.8% to 71.9% on the segment level over the state-of-the-art.

2 Related work

Audio-Visual Learning. Audio-visual learning includes various interesting tasks such as audio-visual representation learning [10, 11, 12, 13, 14, 15, 3, 16], audio-visual event localization [1, 17, 18, 19, 20, 21, 22], audio-visual sound separation [23, 24, 25, 26, 27, 28], audio-visual sound source localization [29, 30, 31, 32], and audio-visual action recognition [33, 34, 35, 36]. Most previous work on these tasks assumes that audio and visual are temporally aligned and always correlated. However, in many videos, audio and visual do not share the same information at a certain time, for instance, something that can be seen is not audible and the sound source is not visible. Therefore, we focus on the audio-visual video parsing task and aim to separately identify the events that happen in each modality with only weakly-supervised video-level labels for training.

Audio-Visual Video Parsing. Audio-visual video parsing (AVVP) task [4] intends to recognize events in each modality and localize their temporal boundaries. Since labeling each modality and segment of a video is time-consuming and labor-intensive, recent work has been conducted in a weakly-supervised manner. Tian *et al.* [4] utilize a hybrid attention network and multiple instance learning mechanism to aggregate segment features into video-level ones. Wu *et al.* [5] adopt the

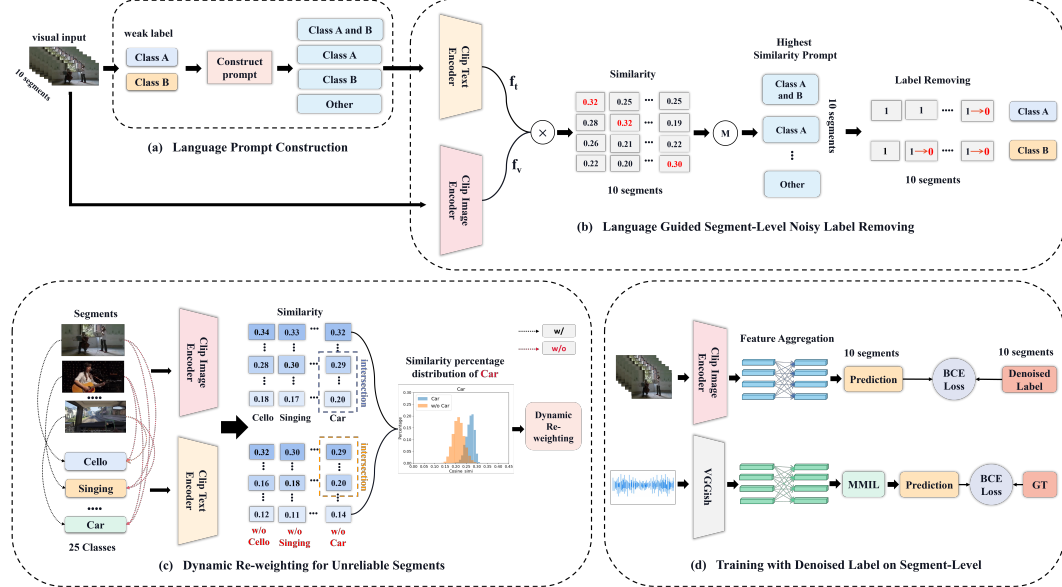


Figure 1: Algorithm Overview. (a) **Language prompts construction** provides prompts for a video to indicate all cases of event appearance based on the weak label of the video. (b) **Language guided segment-Level noisy-label removing** calculates the similarity between prompts and segments, where the prompt with the highest similarity is taken as the segment label. (c) **Dynamic re-weighting for unreliable segments** gathers the segments with and without the event name respectively, then re-weight the segments’ label on the intersection part according to their similarity. (d) **Training with Denoised Label on Segment-Level**. Finally, with denoised segment-level labels, we train the network following [4]. In the figure, “ $\rightarrow 0$ ” denotes label removal, \otimes is the cross product, and “M” denotes the maximum function.

exchange of unrelated video and audio tracks to denoise weakly-supervised labels at the video level. More recently, to explicitly group semantic-aware multi-modal contexts, Mo *et al.* [37] propose a Multi-modal Grouping Network to learn more discriminative audio and visual representations. Chen *et al.* [6] propose a dynamic training mechanism, which lowers the modality-specific noise at the video level. Different from the above approaches, we propose to investigate segment-level label noise. Specifically, we introduce the language modality into the AVVP task and remove noisy labels on the segment level by constructing prompts and calculating the text-image similarity.

Language-Supervised Vision Representation Learning. Language-supervised vision representation learning aims at learning visual representations from language data. Early works for visual representation learning include predicting the bag-of-words representation [38] or training n-gram models [39] on the YFCC100M dataset [40]. While some work like ICMLM [41] and VirTex [42] produce effective visual representations of COCO Captions [43]. Soon after, CLIP [7] quickly draws attention due to its simplicity, scale, and generalization capabilities. CLIP is pre-trained on 400 million image-text pairs using the contrastive learning approach and can be transferred to multi-modal downstream tasks like image caption [44], and video caption [45] due to its zero-shot transfer ability. Thus we employ CLIP as our image encoder to bridge the gap between the image and language descriptions for segment-level label noising.

3 Method

In this paper, we propose a novel Language guided Segment-level Label Denoising (LSLD) method for AVVP, which aims to remove the segment-level noise with the help of natural language. The overview of the proposed method is shown in Fig. 1, where language prompts are generated to calculate the similarity with the segments for denoising. Then dynamic re-weighting is adopted to adjust unreliable segment labels. With the newly assigned segment-level label, the network is trained end-to-end to better classify events on segments.

Following, we introduce our method in detail. We begin with the preliminary and our baseline method (Sec. 3.1). Then we illustrate the language prompt construction (Sec. 3.2), segment-level label denoising (Sec. 3.3), and the dynamic re-weighting strategy (Sec. 3.4).

3.1 Preliminaries

Problem Setup and Notations. Given a T -segments audio-visual video sequence $S = \{V_t, A_t\}_{t=1}^T$, A and V are the audio and visual track, respectively, and each segment is of one second long. Our goal is to predict the event label of each segment in audio and visual, which may contain multiple or no events at all. During *evaluation*, for the t -th video segment (V_t, A_t) , the target is denoted as $(\mathbf{y}_t^a, \mathbf{y}_t^v, \mathbf{y}_t^{av}) \in \mathbb{R}^{1 \times C}$, where \mathbf{y}_t^a , \mathbf{y}_t^v , and \mathbf{y}_t^{av} are labels for audio, visual, and audio-visual events, respectively, and C is the number of event classes. During *training*, we can only obtain the weak label of the video as a whole, which is not specific to modality and segment.

Baseline Framework. To obtain cross-modal and uni-modal information, we adopt HAN [4] as our baseline. HAN [4] extracts visual feature $\mathbf{F}^v = \{\mathbf{f}_t^v\}_{t=1}^T \in \mathbb{R}^{T \times d}$ and audio feature $\mathbf{F}^a = \{\mathbf{f}_t^a\}_{t=1}^T \in \mathbb{R}^{T \times d}$ by Resnet [46] and VGGish [47], where d is the feature dimension. Then it adopts self-attention and cross-attention layers to aggregate cross-modal and uni-modal information at each segment. After gathering the audio and visual features, the segment-level event prediction for audio and visual $(\mathbf{p}_t^a, \mathbf{p}_t^v \in \mathbb{R}^{1 \times C})$ can be obtained through an FC layer and a sigmoid function. Then the video-level prediction is aggregated by attentive MMIL pooling, which is formulated as:

$$\mathbf{p}^a = \sum_{t=1}^T \mathbf{w}_t^a \mathbf{p}_t^a, \quad \mathbf{p}^v = \sum_{t=1}^T \mathbf{w}_t^v \mathbf{p}_t^v, \quad \mathbf{p}^{av} = \sum_{t=1}^T \sum_{m=1}^M \mathbf{W}_t[m] \odot \mathbf{P}_t[m], \quad (1)$$

where $\{\mathbf{w}_t^a, \mathbf{w}_t^v\}$ denote the temporal attention weights, $\mathbf{P}_t = \{\mathbf{p}_t^a, \mathbf{p}_t^v\}$ includes audio and visual predictions, M is the number of modalities. Finally, binary cross-entropy (BCE) loss is adopted to optimize the model in a weakly-supervised way:

$$\mathcal{L}_{base} = \text{BCE}(\mathbf{y}^{av}, \mathbf{p}^{av}) + \text{BCE}(\bar{\mathbf{y}}^a, \mathbf{p}^a) + \text{BCE}(\bar{\mathbf{y}}^v, \mathbf{p}^v), \quad (2)$$

where $\bar{\mathbf{y}}^a$, $\bar{\mathbf{y}}^v$ are video-level audio and visual labels by performing label smooth on \mathbf{y}^{av} to mitigate the impact of noisy labels. As the baseline method only utilize video-level labels during training, which is affected by the segment-level noise, we propose a Language guided Segment-level Label Denoising (LSDL) method to address segment-level noise.

3.2 Language Prompt Construction

As discussed above, during training, we can only access video-level labels, but for each segment, the label could be any combination of events, which is flexible. To address the flexible label assignment challenge, we introduce the language modality into our task, which describes how the events occur. For each video, to consider all cases of event appearance, we create prompts for each case according to its video-level labels. As shown in Fig. 1 (a), taking a video labeled with two classes named A and B as an example, we construct 4 prompts describing A appears, B appears, both classes appear and none of them appear, respectively. Finally, the language prompts for the video could be:

[Class A, Class B, Class A and B, other],

where *other* means no pre-defined event appears.

3.3 Language Guided Segment-Level Label Denoising

With language prompts generated in Sec. 3.2, we intend to remove segment-level noisy labels by language guidance. Specifically, we calculate the similarity between each segment and prompts, where the prompt with the highest similarity is more likely to describe the segment accurately. As illustrated in Fig. 1 (b), we feed the constructed language prompts into CLIP’s text encoder to obtain the text features, and each frame of the video is fed into CLIP’s image encoder to extract the image feature. We denote the text feature as $\mathbf{f}_t \in \mathbb{R}^{N \times d}$ and the visual feature as $\mathbf{f}_v \in \mathbb{R}^{T \times d}$, where N is the number of prompts, T is the number of segments, and d is feature dimension. Then we calculate the text-image similarity matrix $\mathbf{s} \in \mathbb{R}^{N \times T}$ on the normalized text and image feature:

$$\mathbf{s} = \text{Softmax}\left(\frac{\mathbf{f}_t}{\|\mathbf{f}_t\|_2} \otimes \left(\frac{\mathbf{f}_v}{\|\mathbf{f}_v\|_2}\right)^\top\right), \quad (3)$$

where \otimes denotes the matrix multiplication.

With the similarity matrix, the language prompt with the highest similarity for each segment is obtained, which infers the segments' corresponding event label. For instance, as shown in Fig.1 (b), the video is labeled with class A and class B, while the most similar prompt of its second segment is *Class A*, which means that this segment most likely contains only with class A. In this case, we treat class B as the noisy class of this segment for label denoising. Likewise, if the most similar prompt is *other*, both class A and class B will be treated as noisy labels.

With segment-level label denoising, each visual segment is assigned its own event label $\tilde{\mathbf{y}}_t^v$ instead of being regarded as having the same label as the whole video. In this way, the labels depict the visual segments more accurately which boosts network learning.

3.4 Dynamic Re-weighting for Unreliable Segments

In Sec. 3.3, each segment is re-labeled to avoid segment-level noise. However, such noise is inevitable, because some segments may be mislabeled. To further alleviate the impact of mislabeled segments, in this section, we propose to mine the unreliable segments and learn from them with dynamic weight.

To mine the unreliable segments, for each event class, we aggregate the segments with and without the event into two groups (*i.e.*, potentially positive and negative segments) by the denoised segment-level labels. Then, we calculate the similarity between the visual segments and the language prompts of the class for the two groups separately to compare their similarity distribution. We believe that segments containing the event will have relatively high similarity with the event description. The whole process is shown in Fig. 1 (c), where the similarity distributions of with/ without *Car* are presented. We observe that though some segments in orange are labeled as without a *car*, their similarity is still high, while some segments in blue that are labeled as with a *car* are not that similar to the class description. Therefore, we consider the overlap region of the two similarity groups as mislabeled segments.

Then, we propose a dynamic re-weighting strategy to learn unreliable segments softly. Specifically, for an event and a corresponding unreliable segment, the weighted similarity between the segment and event description is adopted as the soft label. Then, for the t -th segment of a video, its label for event class c can be calculated as:

$$\tilde{\mathbf{y}}_t^v[c] = \begin{cases} \text{Min}(1, \alpha \times \mathbf{s}_c), & \tilde{\mathbf{y}}_t^v[c] = 1, \\ \text{Min}(1, \beta \times \mathbf{s}_c), & \tilde{\mathbf{y}}_t^v[c] = 0. \end{cases} \quad (4)$$

where $\text{Min}()$ is a function to return the item with the lowest value, α and β are parameters for the segment with/ without the event c . \mathbf{s}_c is the similarity between segments and class description using Eq. 3. After re-weighting, the unreliable segments labeled without the event c will be assigned a larger value than 0 to consider the appearance of the event. While the unreliable segments labeled with the event c will be assigned a smaller value than 1. Note that, during the application, we set $\alpha > \beta$ to ensure the segments with $\tilde{\mathbf{y}}_t^v[c] = 1$ still have more possibility of the event appearance.

After dynamic re-weighting, we use the segment-level label to optimize the model on the visual segment. The pipeline is shown in Fig. 1 (d). Specifically, we replace the weak label $\bar{\mathbf{y}}^v$ with our segment-level label $\tilde{\mathbf{y}}_t^v$, and replace video-level prediction with segment prediction in Eq. 2. Notably, we also use CLIP to extract the visual features during training since CLIP training from large-scale image-text data and learns richer visual information.

4 Experiments

4.1 Experimental Setup

Dataset. In the AVVP task, we evaluate our method on the Look, Listen and Parse (LLP) Dataset [4]. The dataset contains 11,849 video clips of 10-seconds long from 25 different event categories, including human activities, animals, musical instruments, *etc*. For the training process, we use 10,000 video clips with only video-level event labels. The remaining 1849 validation and test videos possess modality and segment-specific labels (*i.e.*, start and end time of each event on audio and visual track). We conduct experiments following the official data splits from the LLP dataset.

Evaluation Metrics. We evaluate the parsing performance of audio, visual, and audio-visual events under both segment-level and event-level metrics by adopting F-scores. The segment-level metrics can

Table 1: **Comparisons with the state-of-the-art methods on LLP.** “Clip” means we reproduced the method with the visual feature extracted from CLIP, while * represents our baseline framework. The last 3 lines are all label denoising methods developed on the HAN [4] framework. The best results are marked in bold.

Method	Segment-Level					Event-level				
	A	V	A-V	Type	Event	A	V	A-V	Type	Event
AVE [1]	47.2	37.1	35.4	39.9	41.6	40.4	34.7	31.6	35.5	36.5
AVSDN [17]	47.8	52.0	37.1	45.7	50.8	34.1	46.3	26.5	35.6	37.7
HAN [4]*	60.1	52.9	48.9	54.0	55.4	51.3	48.9	43.0	47.7	48.0
MGN [37]	60.8	55.4	50.4	55.5	57.2	51.1	52.4	44.4	49.3	49.1
MA [5]	60.3	60.0	55.1	58.9	57.9	53.6	56.4	49.0	53.0	50.6
JoMoLD [6]	61.3	63.8	57.2	60.8	59.9	53.9	59.9	49.6	54.5	52.5
HAN + Clip *	62.4	55.6	51.3	56.4	57.5	53.9	51.7	44.5	50.0	51.6
MGN + Clip	61.0	60.0	53.8	58.3	58.9	50.8	56.7	47.3	51.6	50.2
MA + Clip	60.0	65.1	57.2	60.8	59.6	51.7	61.7	49.2	54.2	52.4
JoMoLD + Clip	62.6	67.1	59.1	62.9	61.4	54.6	63.5	50.7	56.3	54.0
LSLD (ours)	62.3	71.9	63.4	65.9	62.5	53.0	68.8	55.9	59.3	53.7

Table 2: Ablation study of each component of LSLD. Here, “DeN” denotes language-guided segment-level label denoising. “ReW” denotes the dynamic weighting strategy on unreliable segments.

DeN	ReW	Segment-Level					Event-level				
		A	V	A-V	Type	Event	A	V	A-V	Type	Event
✗	✗	62.4	55.6	51.3	56.4	57.5	53.9	51.7	44.5	50.0	51.6
✓	✗	62.5	70.6	62.1	65.1	62.4	53.2	67.0	54.0	58.1	53.5
✓	✓	62.3	71.9	63.4	65.9	62.5	53.0	68.8	55.9	59.3	53.7

evaluate segment-wise event prediction performance. For the event-level metrics, we extract events by concatenating consecutive positive segments in the same event and compute event-level F-score with mIoU=0.5 as the threshold. In addition, we evaluate the parsing performance of audio-visual events using Type@AV and Event@AV metrics. Type@AV is calculated by averaging audio, visual, and audio-visual event evaluation results while Event@AV considers all audio and visual event categories for each sample instead of directly averaging results from different events.

Implementation Details. We conduct the training and evaluation processes on a single NVIDIA GTX 2080 Ti GPU with 11 GB memory. Following the data preprocessing in previous works, we decode a 10-second video at 8 fps into 10 segments. Instead of using pre-trained ResNet-152 [46] and R(2+1)D [48], we utilize CLIP’s [7] image encoder (*i.e.*, pre-trained ViT-B/16 [49]) to extract segment features with richer semantic information. Furthermore, we leverage VGGish [47] pre-trained on AudioSet [50] to extract the audio features. For a fair comparison, we also reproduce existing methods [4, 5, 37, 6] with the visual features extracted by CLIP. Following HAN [4] we adopt the Adam optimizer and the learning rate 6e-4 drops by a factor of 0.25 for every 6 epochs. We train the model with a batch size of 32 for 20 epochs.

4.2 Comparison with State-of-the-art Methods

To demonstrate the effectiveness of our method, we compare it to several baseline works including the audio-visual event localization approach AVE [1] and AVSDN [17] and the state-of-the-art methods for the weakly-AVVP task, such as HAN [4], MA [5], JoMoLD [6], *etc.* To compare more fairly, we also apply the visual features extracted from CLIP [7] to previous works of the AVVP task.

As shown in Table 1, we conduct our experiments on the LLP dataset with all state-of-the-art methods. We observe that our method has competitive performance on all evaluation metrics. Compared with our baseline method HAN [4] with Clip, the proposed method can significantly improve the performances on visual metrics. Especially, our method gains 16.3 and 12.1 points on segment-level

Table 3: Analysis of different strategies to indicate that no event appears in the prompt.

Method	Segment-Level					Event-level				
	A	V	A-V	Type	Event	A	V	A-V	Type	Event
[Class, Not Class]	61.8	58.4	54.8	58.3	57.9	52.5	55.6	49.6	52.6	50.2
[Class, None]	62.0	71.0	62.8	65.3	62.1	53.0	67.9	55.1	58.7	53.4
[Class, Other]	62.3	71.9	63.4	65.9	62.5	53.0	68.8	55.9	59.3	53.7

Table 4: Algorithm analysis of dynamic re-weighting. All results are of visual metric.

(a) Analysis on different α and β values.

$\alpha \backslash \beta$	0.2	0.4	0.6	0.8
3	68.1	68.3	69.0	69.7
3.5	70.7	69.2	71.4	71.2
4	71.0	71.9	71.6	70.5
4.5	70.7	70.2	71.4	70.7

(b) Analysis of different re-weighting strategies.

Method	Visual	
	Segment-Level	Event-Level
re-weight on w/ event	69.9	66.5
re-weight on w/o event	70.4	67.2
stable re-weight	71.2	67.2
dynamic re-weight	71.9	68.8

visual parsing and audio-visual parsing, respectively. Similar improvements are also observed on event-level tasks.

Compared with state-of-the-art methods with Clip, our method still yields better performance on all visual-related metrics. Especially, compared with JoMoLD+Clip, we achieve 4.8, 4.3, and 3.0 points of improvement in terms of segment-level visual, audio-visual, and type parsing. On the other hand, although we do not conduct denoising on the audio track, our results on audio parsing are only 0.3 points slightly lower than JoMoLD+Clip, in terms of segment level.

4.3 Ablation Studies

Effectiveness of language guided segment-level denoising. The ablation study of denoising is shown in Table 2. We observe that the results on visual parsing are improved by 15% and 15.3% on segment-level and event-level, respectively when we construct prompts and remove segment-level noisy labels by language guidance. The significant improvement demonstrates that with the help of language description, our method does provide more accurate segment-level labels for the visual track, which enhances network learning.

Analysis of different types of prompts. As shown in Table 3, we investigate the influence of using different language descriptions to express that no event appears in the segment. We observe that when using prompts like [Class, Not Class], the performance is much lower than our method. We suspect the reason is that the text encoder is more sensitive to meaningful words like event class while neglecting the negative word *not*. When using *none*, the result in visual metrics is about 1 point lower than ours. The reason is that though the pre-defined events do not appear, background scenes like sky and trees may exist. When using the description *other*, we obtain the best performance, where we neither throw away the possibility of the appearance of background classes nor introduce event categories that do not appear.

Effectiveness of dynamic re-weighting. The ablation study of dynamic re-weighting is shown in Table 2. We observe that the results on visual parsing are improved by 1.3% and 1.8% on segment-level and event-level, respectively. The improvement demonstrates that our method accurately finds the possible mislabeled segment to learn them softly.

Analysis of different α and β values. According to Eq. 4, the hyper-parameter α and β are used to be multiplied with similarity to be served as the weight for unreliable segments with/ without the event, respectively. In Table 4 (a), as α becomes bigger, the results are usually improved, as our denoising method identifies most of the segments into the correct category, so a larger weight should be given. However, when α is too big, the performance drops, because most of the labels will remain at 1 without any re-weighting to unreliable segments. A similar observation is found in β .

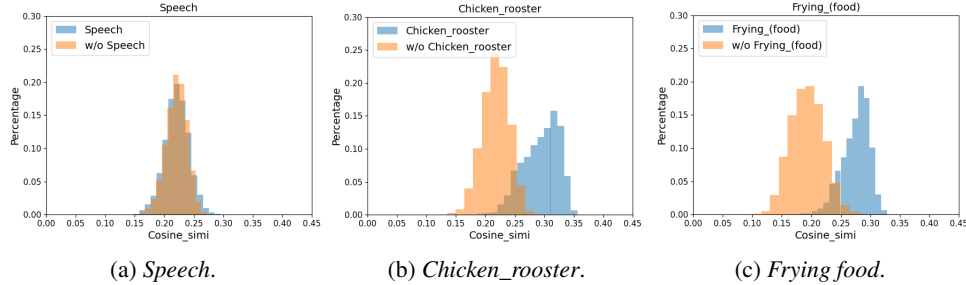


Figure 2: Similarity percentage distribution. The similarity is calculated between the visual segments and the event description. We split the segments into with (blue)/ without (yellow) the event. Examples for three events are shown.

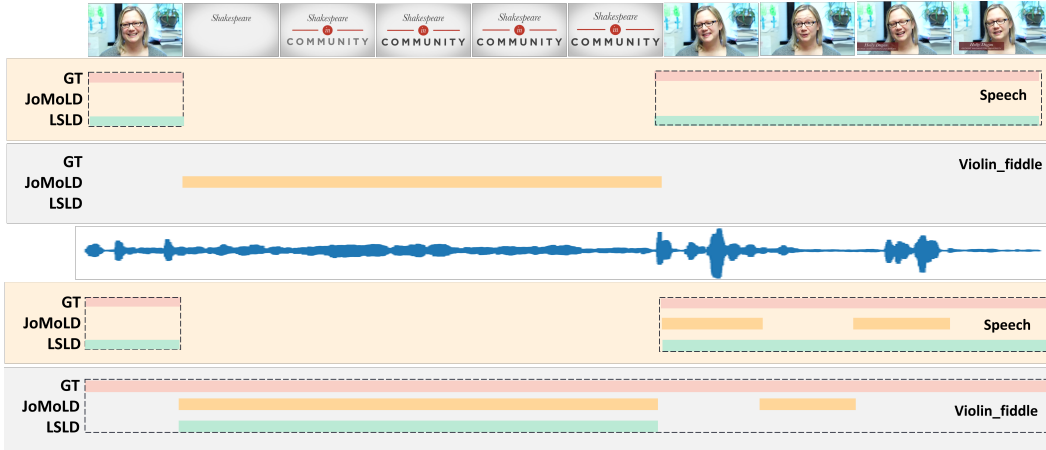


Figure 3: Qualitative result on the LLP test set. The results of our method (LSID) and the state-of-the-art method JoMoLD [6] are shown. “GT” denotes the ground truth annotations.

Analysis of different re-weighting strategies. As shown in Table 4 (b), four different strategies are compared. The first two rows denote conducting dynamic re-weighting on only segments with or without the event, where the results are 1.3% and 2.0% lower than ours, respectively. “stable re-weight” denotes using stable value instead of dynamic similarity to calculate weight, where we find the results are 0.7% and 1.6% lower than ours in terms of segment-level and event-level. This demonstrates that since segments with higher similarity are more likely to belong to the category, re-weighting with dynamic similarity helps to better learn the unreliable segments.

In addition, we visualize three examples of similarity distribution with/ without an event in Fig. 2. We observe that in most cases, such as *chicken rooster* and *frying food*, the similarity distribution is well separated, while only a small area is taken as unreliable segments. However, there is a special case, *speech*, where we can hardly recognize whether it happens through the similarity with the language prompt of the class. We suspect the reason is that *speech* is difficult to recognize in vision. For example, the vision is about a basketball game while *speech* could only occur in the audio track.

4.4 Qualitative Results

Visualization of video parsing results. We compare our method with the SOTA method JoMoLD [6] by visualizing the audio and visual parsing results in Fig. 3. As for the visual parsing task, the visual track only contains *speech* on the segments, where JoMoLD recognizes it as the *Violin_fiddle*, and our method identifies the *speech* event and localizes the temporal boundaries correctly. The results prove that our approach is more effective in recognizing events in visual segments. As for the audio parsing task, our LSID properly identifies the segments with *speech*, yet JoMoLD only recognizes *speech* on some of the segments. This demonstrates that though LSID only conducts denoising on the visual track, there is a potential connection between audio and visual, so we are capable of identifying the



Figure 4: Visualization of segment-level label denoising on visual track. The similarity between our prompts and segments are presented. Results on JoMoLD [6] and our method are shown. Each example presents three segments of a video.

events that appear on the audio segment as well. However, when identifying the *Violin_fiddle*, both LSLLD and JoMoLD only recognize the event in some segments due to the interference of the speech voice, which impels us to further refine the method on the audio modality.

Visualization of the denoising procedure. We visualize the segment-level label denoising results of our method and JoMoLD [6] in Fig. 4. We observe that, in all examples, our prompt of the highest similarity captures the appeared events accurately. As shown in Fig. 4 (a), in the last two segments there is no event exists, where JoMoLD still recognizes *Car* because *Car* appears in the first segment and JoMoLD can only denoise at video-level. In contrast, LSLLD correctly assigns labels for all the segments. In Fig. 4 (b), LSLLD recognizes different event appearances on the segment level, while JoMoLD fails to do so, which demonstrates the importance of segment-specific label assignment and the effectiveness of our method. In Fig. 4 (c), LSLLD successfully removes *Singing* on the first segment, yet JoMoLD is unable to remove it. A similar observation could be found in Fig. 4 (d).

5 Conclusion and Discussion

In this paper, we address the weakly-supervised audio-visual video parsing task. Instead of focusing on the overall video instance level denoising, we propose to assign specific segment-level labels for each video on the visual track. Since each segment label is not predefined but could be any combination of events that occur in the video, we introduce the language modality into our task and construct language prompts to represent all cases of event appearance. The similarities between each segment and prompts are calculated, where the prompt with the highest similarity is considered the segment-level label. To further alleviate the effect of segment-level label noise, we apply dynamic weighting on segments that may be mislabeled. Extensive experiments and qualitative results show that our method outperforms the state-of-the-art methods on the visual metrics by a large margin.

Limitation. Although we successfully assigned segment-level labels for the visual track for training and achieved significant improvement, the audio track remains the vague weak label. However, it is hard to assign segment-level labels for audio since the existing audio-language models [8, 9] are usually trained on a small amount of data and can only recognize video-level events, which is powerless on segment-level prediction. In future work, more effort will be made to segment-level audio learning.

Broader impact. Audio-Visual Video Parsing (AVVP) has numerous potential real-life applications, such as professional media production, audiovisual archive management, entertainment, and so on. Our method provides a new perspective to address AVVP, *i.e.*, through the guidance of natural language, which could benefit from large-scale vision-language models and will inspire future works.

References

- [1] Yapeng Tian, Jing Shi, Bochen Li, Zhiyao Duan, and Chenliang Xu. Audio-visual event localization in unconstrained videos. In *Proceedings of the European Conference on Computer Vision (ECCV)*, pages 247–263, 2018.
- [2] Di Hu, Feiping Nie, and Xuelong Li. Deep multimodal clustering for unsupervised audiovisual learning. In *Proceedings of the IEEE/CVF Conference on Computer Vision and Pattern Recognition*, pages 9248–9257, 2019.
- [3] Pedro Morgado, Nuno Vasconcelos, and Ishan Misra. Audio-visual instance discrimination with cross-modal agreement. In *Proceedings of the IEEE/CVF Conference on Computer Vision and Pattern Recognition*, pages 12475–12486, 2021.
- [4] Yapeng Tian, Dingzeyu Li, and Chenliang Xu. Unified multisensory perception: Weakly-supervised audio-visual video parsing. In *Proceedings of the European Conference on Computer Vision (ECCV)*, pages 436–454, 2020.
- [5] Yu Wu and Yi Yang. Exploring heterogeneous clues for weakly-supervised audio-visual video parsing. In *Proceedings of the IEEE/CVF Conference on Computer Vision and Pattern Recognition*, pages 1326–1335, 2021.
- [6] Haoyue Cheng, Zhaoyang Liu, Hang Zhou, Chen Qian, Wayne Wu, and Limin Wang. Joint-modal label denoising for weakly-supervised audio-visual video parsing. In *Proceedings of the European Conference on Computer Vision (ECCV)*, pages 431–448, 2022.
- [7] Alec Radford, Jong Wook Kim, Chris Hallacy, Aditya Ramesh, Gabriel Goh, Sandhini Agarwal, Girish Sastry, Amanda Askell, Pamela Mishkin, Jack Clark, et al. Learning transferable visual models from natural language supervision. In *International conference on machine learning*, pages 8748–8763, 2021.
- [8] Benjamin Elizalde, Soham Deshmukh, Mahmoud Al Ismail, and Huaming Wang. Clap learning audio concepts from natural language supervision. In *ICASSP 2023-2023 IEEE International Conference on Acoustics, Speech and Signal Processing (ICASSP)*, pages 1–5, 2023.
- [9] Ilaria Manco, Emmanouil Benetos, Elio Quinton, and György Fazekas. Contrastive audio-language learning for music. *arXiv preprint arXiv:2208.12208*, 2022.
- [10] Yusuf Aytar, Carl Vondrick, and Antonio Torralba. Soundnet: Learning sound representations from unlabeled video. *Advances in neural information processing systems*, 2016.
- [11] Saurabh Gupta, Judy Hoffman, and Jitendra Malik. Cross modal distillation for supervision transfer. In *Proceedings of the IEEE conference on computer vision and pattern recognition*, pages 2827–2836, 2016.
- [12] Relja Arandjelovic and Andrew Zisserman. Look, listen and learn. In *Proceedings of the IEEE international conference on computer vision*, pages 609–617, 2017.
- [13] Bruno Korbar, Du Tran, and Lorenzo Torresani. Cooperative learning of audio and video models from self-supervised synchronization. *Advances in Neural Information Processing Systems*, 2018.
- [14] Humam Alwassel, Dhruv Mahajan, Bruno Korbar, Lorenzo Torresani, Bernard Ghanem, and Du Tran. Self-supervised learning by cross-modal audio-video clustering. *Advances in Neural Information Processing Systems*, pages 9758–9770, 2020.
- [15] Pedro Morgado, Yi Li, and Nuno Vasconcelos. Learning representations from audio-visual spatial alignment. *Advances in Neural Information Processing Systems*, pages 4733–4744, 2020.
- [16] Yuan Gong, Andrew Rouditchenko, Alexander H Liu, David Harwath, Leonid Karlinsky, Hilde Kuehne, and James R Glass. Contrastive audio-visual masked autoencoder. In *The Eleventh International Conference on Learning Representations*, 2022.

- [17] Yan-Bo Lin, Yu-Jhe Li, and Yu-Chiang Frank Wang. Dual-modality seq2seq network for audio-visual event localization. In *ICASSP 2019-2019 IEEE International Conference on Acoustics, Speech and Signal Processing (ICASSP)*, pages 2002–2006, 2019.
- [18] Yu Wu, Linchao Zhu, Yan Yan, and Yi Yang. Dual attention matching for audio-visual event localization. In *Proceedings of the IEEE/CVF international conference on computer vision*, pages 6292–6300, 2019.
- [19] Jinxing Zhou, Liang Zheng, Yiran Zhong, Shijie Hao, and Meng Wang. Positive sample propagation along the audio-visual event line. In *Proceedings of the IEEE/CVF Conference on Computer Vision and Pattern Recognition*, pages 8436–8444, 2021.
- [20] Yan Xia and Zhou Zhao. Cross-modal background suppression for audio-visual event localization. In *Proceedings of the IEEE/CVF Conference on Computer Vision and Pattern Recognition*, pages 19989–19998, 2022.
- [21] Varshanth Rao, Md Ibrahim Khalil, Haoda Li, Peng Dai, and Juwei Lu. Dual perspective network for audio-visual event localization. In *Proceedings of the European Conference on Computer Vision (ECCV)*, pages 689–704, 2022.
- [22] Tanvir Mahmud and Diana Marculescu. Ave-clip: Audioclip-based multi-window temporal transformer for audio visual event localization. In *Proceedings of the IEEE/CVF Winter Conference on Applications of Computer Vision*, pages 5158–5167, 2023.
- [23] Ariel Ephrat, Inbar Mosseri, Oran Lang, Tali Dekel, Kevin Wilson, Avinatan Hassidim, William T Freeman, and Michael Rubinstein. Looking to listen at the cocktail party: A speaker-independent audio-visual model for speech separation. *arXiv preprint arXiv:1804.03619*, 2018.
- [24] Hang Zhao, Chuang Gan, Andrew Rouditchenko, Carl Vondrick, Josh McDermott, and Antonio Torralba. The sound of pixels. In *Proceedings of the European conference on computer vision (ECCV)*, pages 570–586, 2018.
- [25] Hang Zhou, Xudong Xu, Dahua Lin, Xiaogang Wang, and Ziwei Liu. Sep-stereo: Visually guided stereophonic audio generation by associating source separation. In *Proceedings of the European Conference on Computer Vision (ECCV)*, pages 52–69, 2020.
- [26] Ruohan Gao and Kristen Grauman. Visualvoice: Audio-visual speech separation with cross-modal consistency. In *2021 IEEE/CVF Conference on Computer Vision and Pattern Recognition (CVPR)*, pages 15490–15500, 2021.
- [27] Sagnik Majumder, Ziad Al-Halah, and Kristen Grauman. Move2hear: Active audio-visual source separation. In *Proceedings of the IEEE/CVF International Conference on Computer Vision*, pages 275–285, 2021.
- [28] Efthymios Tzinis, Scott Wisdom, Tal Remez, and John R Hershey. Audioscopev2: Audio-visual attention architectures for calibrated open-domain on-screen sound separation. In *Proceedings of the European Conference on Computer Vision (ECCV)*, pages 368–385, 2022.
- [29] Arda Senocak, Tae-Hyun Oh, Junsik Kim, Ming-Hsuan Yang, and In So Kweon. Learning to localize sound source in visual scenes. In *Proceedings of the IEEE Conference on Computer Vision and Pattern Recognition*, pages 4358–4366, 2018.
- [30] Relja Arandjelovic and Andrew Zisserman. Objects that sound. In *Proceedings of the European conference on computer vision (ECCV)*, pages 435–451, 2018.
- [31] Rui Qian, Di Hu, Heinrich Dinkel, Mengyue Wu, Ning Xu, and Weiyao Lin. Multiple sound sources localization from coarse to fine. In *Proceedings of the European Conference on Computer Vision (ECCV)*, pages 292–308, 2020.
- [32] Hanyu Xuan, Zhiliang Wu, Jian Yang, Yan Yan, and Xavier Alameda-Pineda. A proposal-based paradigm for self-supervised sound source localization in videos. In *Proceedings of the IEEE/CVF Conference on Computer Vision and Pattern Recognition*, pages 1029–1038, 2022.

[33] Fanyi Xiao, Yong Jae Lee, Kristen Grauman, Jitendra Malik, and Christoph Feichtenhofer. Audiovisual slowfast networks for video recognition. *arXiv preprint arXiv:2001.08740*, 2020.

[34] Ruohan Gao, Tae-Hyun Oh, Kristen Grauman, and Lorenzo Torresani. Listen to look: Action recognition by previewing audio. In *Proceedings of the IEEE/CVF Conference on Computer Vision and Pattern Recognition*, pages 10457–10467, 2020.

[35] Rameswar Panda, Chun-Fu Richard Chen, Quanfu Fan, Ximeng Sun, Kate Saenko, Aude Oliva, and Rogerio Feris. Adamml: Adaptive multi-modal learning for efficient video recognition. In *Proceedings of the IEEE/CVF International Conference on Computer Vision*, pages 7576–7585, 2021.

[36] Saghir Alafasly, Jian Lu, Chen Xu, and Yuru Zou. Learnable irrelevant modality dropout for multimodal action recognition on modality-specific annotated videos. In *Proceedings of the IEEE/CVF Conference on Computer Vision and Pattern Recognition*, pages 20208–20217, 2022.

[37] Shentong Mo and Yapeng Tian. Multi-modal grouping network for weakly-supervised audio-visual video parsing. In *Advances in Neural Information Processing Systems*, 2022.

[38] Armand Joulin, Laurens Van Der Maaten, Allan Jabri, and Nicolas Vasilache. Learning visual features from large weakly supervised data. In *Proceedings of the European Conference on Computer Vision (ECCV)*, pages 67–84, 2016.

[39] Ang Li, Allan Jabri, Armand Joulin, and Laurens Van Der Maaten. Learning visual n-grams from web data. In *Proceedings of the IEEE International Conference on Computer Vision*, pages 4183–4192, 2017.

[40] Bart Thomée, David A Shamma, Gerald Friedland, Benjamin Elizalde, Karl Ni, Douglas Poland, Damian Borth, and Li-Jia Li. Yfcc100m: The new data in multimedia research. *Communications of the ACM*, (2):64–73, 2016.

[41] Mert Bulent Sariyildiz, Julien Perez, and Diane Larlus. Learning visual representations with caption annotations. In *Proceedings of the European Conference on Computer Vision (ECCV)*, pages 153–170, 2020.

[42] Karan Desai and Justin Johnson. Virtex: Learning visual representations from textual annotations. In *Proceedings of the IEEE/CVF conference on computer vision and pattern recognition*, pages 11162–11173, 2021.

[43] Xinlei Chen, Hao Fang, Tsung-Yi Lin, Ramakrishna Vedantam, Saurabh Gupta, Piotr Dollár, and C Lawrence Zitnick. Microsoft coco captions: Data collection and evaluation server. *arXiv preprint arXiv:1504.00325*, 2015.

[44] Manuele Barraco, Marcella Cornia, Silvia Cascianelli, Lorenzo Baraldi, and Rita Cucchiara. The unreasonable effectiveness of clip features for image captioning: an experimental analysis. In *proceedings of the IEEE/CVF conference on computer vision and pattern recognition*, pages 4662–4670, 2022.

[45] Mingkang Tang, Zhanyu Wang, Zhenhua Liu, Fengyun Rao, Dian Li, and Xiu Li. Clip4caption: Clip for video caption. In *Proceedings of the 29th ACM International Conference on Multimedia*, pages 4858–4862, 2021.

[46] Kaiming He, Xiangyu Zhang, Shaoqing Ren, and Jian Sun. Deep residual learning for image recognition. In *Proceedings of the IEEE conference on computer vision and pattern recognition*, pages 770–778, 2016.

[47] Shawn Hershey, Sourish Chaudhuri, Daniel PW Ellis, Jort F Gemmeke, Aren Jansen, R Channing Moore, Manoj Plakal, Devin Platt, Rif A Saurous, Bryan Seybold, et al. Cnn architectures for large-scale audio classification. In *2017 ieee international conference on acoustics, speech and signal processing (icassp)*, pages 131–135, 2017.

[48] Du Tran, Heng Wang, Lorenzo Torresani, Jamie Ray, Yann LeCun, and Manohar Paluri. A closer look at spatiotemporal convolutions for action recognition. In *Proceedings of the IEEE conference on Computer Vision and Pattern Recognition*, pages 6450–6459, 2018.

- [49] Alexey Dosovitskiy, Lucas Beyer, Alexander Kolesnikov, Dirk Weissenborn, Xiaohua Zhai, Thomas Unterthiner, Mostafa Dehghani, Matthias Minderer, Georg Heigold, Sylvain Gelly, et al. An image is worth 16x16 words: Transformers for image recognition at scale. *arXiv preprint arXiv:2010.11929*, 2020.
- [50] Jort F Gemmeke, Daniel PW Ellis, Dylan Freedman, Aren Jansen, Wade Lawrence, R Channing Moore, Manoj Plakal, and Marvin Ritter. Audio set: An ontology and human-labeled dataset for audio events. In *2017 IEEE international conference on acoustics, speech and signal processing (ICASSP)*, pages 776–780, 2017.
- [51] Jiashuo Yu, Ying Cheng, Rui-Wei Zhao, Rui Feng, and Yuejie Zhang. Mm-pyramid: Multi-modal pyramid attentional network for audio-visual event localization and video parsing. In *Proceedings of the 30th ACM International Conference on Multimedia*, pages 6241–6249, 2022.
- [52] Xun Jiang, Xing Xu, Zhiguo Chen, Jingran Zhang, Jingkuan Song, Fumin Shen, Huimin Lu, and Heng Tao Shen. Dhnn: Dual hierarchical hybrid network for weakly-supervised audio-visual video parsing. In *Proceedings of the 30th ACM International Conference on Multimedia*, pages 719–727, 2022.

Appendix

In the supplementary material, we first conduct more ablation studies for our method in Sec. A. In Sec. B, we provide more examples of the similarity distribution with/without the event and visualize more label denoising cases to validate the effectiveness of our method. In addition, we provide videos to show the audio-visual parsing results and provide the code for the method implementation.

A More Ablation Studies

In this section, we conduct more ablation studies on the proposed method, including performing our method on different baseline frameworks, studying the impact of changing class names to make the constructed prompt more contextual and the effectiveness of only using visual features extracted by CLIP [7] during training.

Effectiveness with different baselines. To investigate the flexibility of our approach, we apply our method to different baseline frameworks for the AVVP task. As illustrated in Table 5, the results of all networks are improved on both audio and visual metrics with our method, especially on the segment-level visual metric, which is 10 points higher than using extracted features by CLIP. The experiments show that our denoised labels are indeed influential and can be properly employed on different baseline frameworks.

Table 5: Apply our method to different state-of-the-art methods for the AVVP task. “Clip” means we reproduce the method with the visual feature extracted from CLIP.

Method	Segment-Level					Event-level				
	A	V	A-V	Type	Event	A	V	A-V	Type	Event
MM-Pyramid [51]	60.9	54.4	50.0	55.1	57.6	52.7	51.8	44.4	49.9	50.5
MM-Pyramid + Clip	62.8	56.3	51.6	56.9	60.0	53.1	52.2	45.5	50.3	50.7
MM-Pyramid + LSLD	63.3	66.8	60.4	63.5	62.4	54.5	62.5	52.6	56.5	53.2
DHHN [52]	61.3	58.3	52.9	57.5	58.1	54.0	55.1	47.3	51.5	51.5
DHHN + Clip	62.6	59.1	53.4	58.4	59.1	54.3	55.2	46.8	52.1	52.5
DHHN + LSLD	64.1	69.0	60.7	64.6	64.0	56.2	66.2	53.7	58.7	56.4

Effectiveness of modifying class names in prompts. In the implementation, we try to modify the prompts to make them more natural instead of using pure event class names. From the results in Table 6, we can see that the segment-level visual metric improves by 1.5 points when we add *playing* before the class names related to musical instruments and replace *basketball bounce* with *playing basketball*. As we transform objects like *Accordion* into human behavior (i.e. *playing the Accordion*), the prompt becomes more natural when they are connected with events related to human actions. For instance, we change *Singing and Accordion* into *Singing and playing the Accordion*. Furthermore, our approach is much better than the one that adds *a photo of* before the prompt since the result of the segment level is 1.8 points higher. While adding *a person* before the class related to human activity would make the prompt more natural, for example, *a person speeching and playing the guitar*, *a person* would introduce a new category (i.e. person) to the sentence, so it is better to add only action-related words as in our method.

Table 6: Study the impact of varying class names to make the prompt more contextual. only visual metrics are reported for more explicit comparisons.

Class Description	Visual	
	Segment-Level	Event-Level
Original Class Desc	70.4	67.2
Desc + playing	71.9	68.8
Desc + a photo of	70.1	66.5
Desc + playing + a person	69.4	66.0

Table 7: Study the effectiveness of only using CLIP’s Image Encoder to extract visual features when training.

Method	Segment-Level					Event-level				
	A	V	A-V	Type	Event	A	V	A-V	Type	Event
Resnet [46] 2D + 3D	57.3	59.5	52.9	56.6	55.5	47.8	56.9	47.1	50.6	46.3
CLIP (ViT-B/32) + 3D	61.9	68.5	61.1	63.8	61.4	52.5	65.3	53.4	57.1	52.3
CLIP (ViT-B/16) + 3D	61.8	69.5	61.8	64.4	61.4	52.0	66.2	54.1	57.4	52.1
CLIP (ViT-B/32) only	61.5	70.4	61.6	64.5	61.9	52.5	67.2	54.1	58.0	53.4
CLIP (ViT-B/16) only	62.3	71.9	63.4	65.9	62.5	53.0	68.8	55.9	59.3	53.7

Effectiveness of only using visual features extracted by CLIP. In Table 7, we can see that when we use the features extracted by CLIP during training, we improve the visual metrics by 12.4 points on the segment level, which shows that CLIP can extract richer visual information from the image. Also, the segment-level audio metric is improved by 5 points since there is a natural connection between audio and visual. Furthermore, when we use ViT/B-16 [49] as the image encoder, the result is 1.5 points higher than ViT/B-32 on the segment-level visual metric, indicating that the extracted visual features are better when we divide the images into more patches. Finally, we find that rich visual information can be obtained by only using CLIP since the result on segment-level visual metrics drops by 2.4 points when combines with R(2+1)D [48].

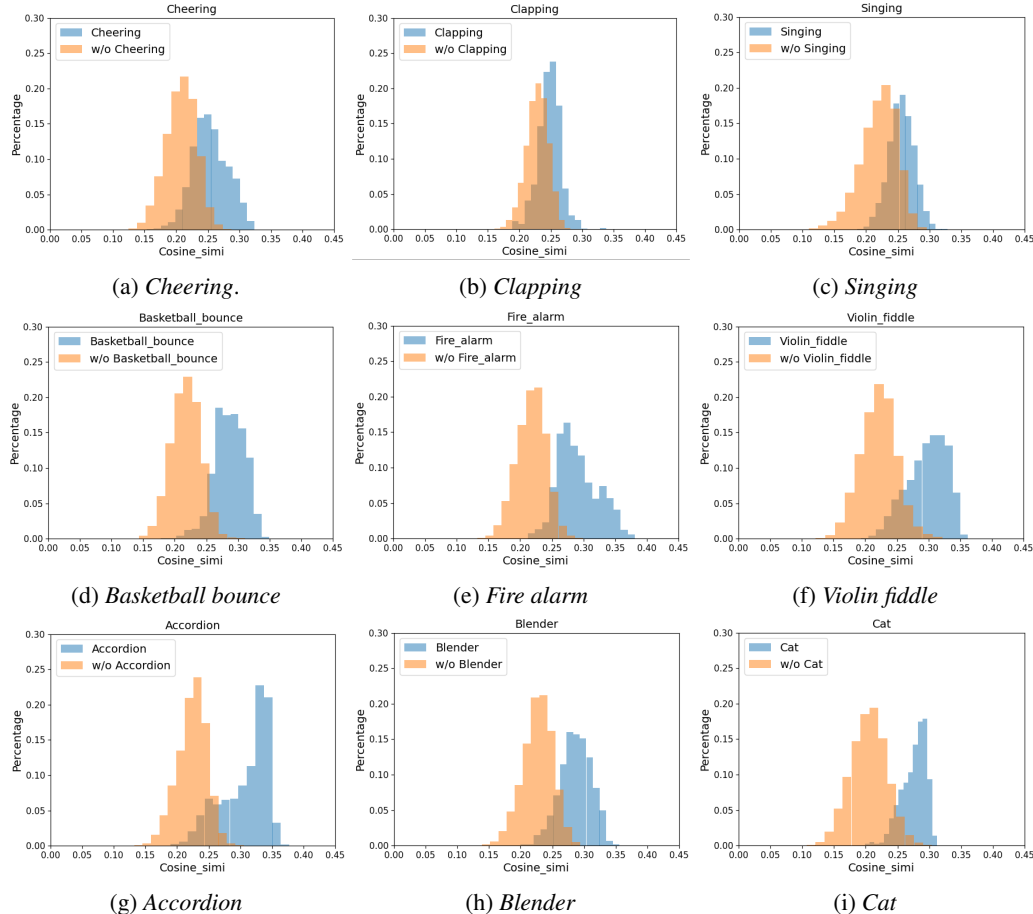


Figure 5: Similarity percentage distribution. The similarity is calculated between the visual segments and the event description. We split the segments into with (blue)/ without (yellow) the event.

B Additional Qualitative Analyses

In this section, we visualize more cases of similarity percentage distribution with or without the event and perform more examples of the label denoising procedure.

Visualization of similarity percentage distribution. As shown in Figure 5, we can observe that the intersection area on sound-related events is relatively large. We argue that identifying events like *Singing* is more difficult as it requires observation of human facial micro-expressions. Conversely, the model will be more accurate when it comes to recognizing obvious objects or animals like *basketball*, *fire alarm*, *Cat*, *Blender*, etc. Thus, we need to perform dynamic re-weighting on the segments with unreliable labels, especially for sound-related events.

Visualization of segment-level label denoising cases. In Figure 6 and Figure 7, we present several visualization results of the label denoising process. For a more comprehensive analysis of the effectiveness of our approach, we visualize the label assignment of various event categories, such as *Fire alarm*, *Helicopter*, *Clapping*, etc. We can observe in Figure 6 (a), JoMoLD [6] removes *speech* on the video-level label while *speech* appears in several segments. In Figure 6 (b), there is no one *Singing* in the first 2 segments, yet JoMoLD still recognizes *Singing* since it can only denoise at video-level, and LSLLD correctly assigns the right label for the segments. A similar observation can be found in Figure 6 (c), (d), (e). Note that, we cannot assign the *Car* label to the segments in Figure 6 (c) because “GT” does not contain it. As shown in Figure 6 (f), LSLLD recognizes *Speech* and only removes *Clapping* for the first 2 segments, while JoMoLD fails to do so.



Figure 6: Visualization of segment-level label denoising on visual track. The similarity between our prompts and segments are presented. Results on JoMoLD and our method are shown. Each example presents three segments of a video. “GT” denotes the ground truth.

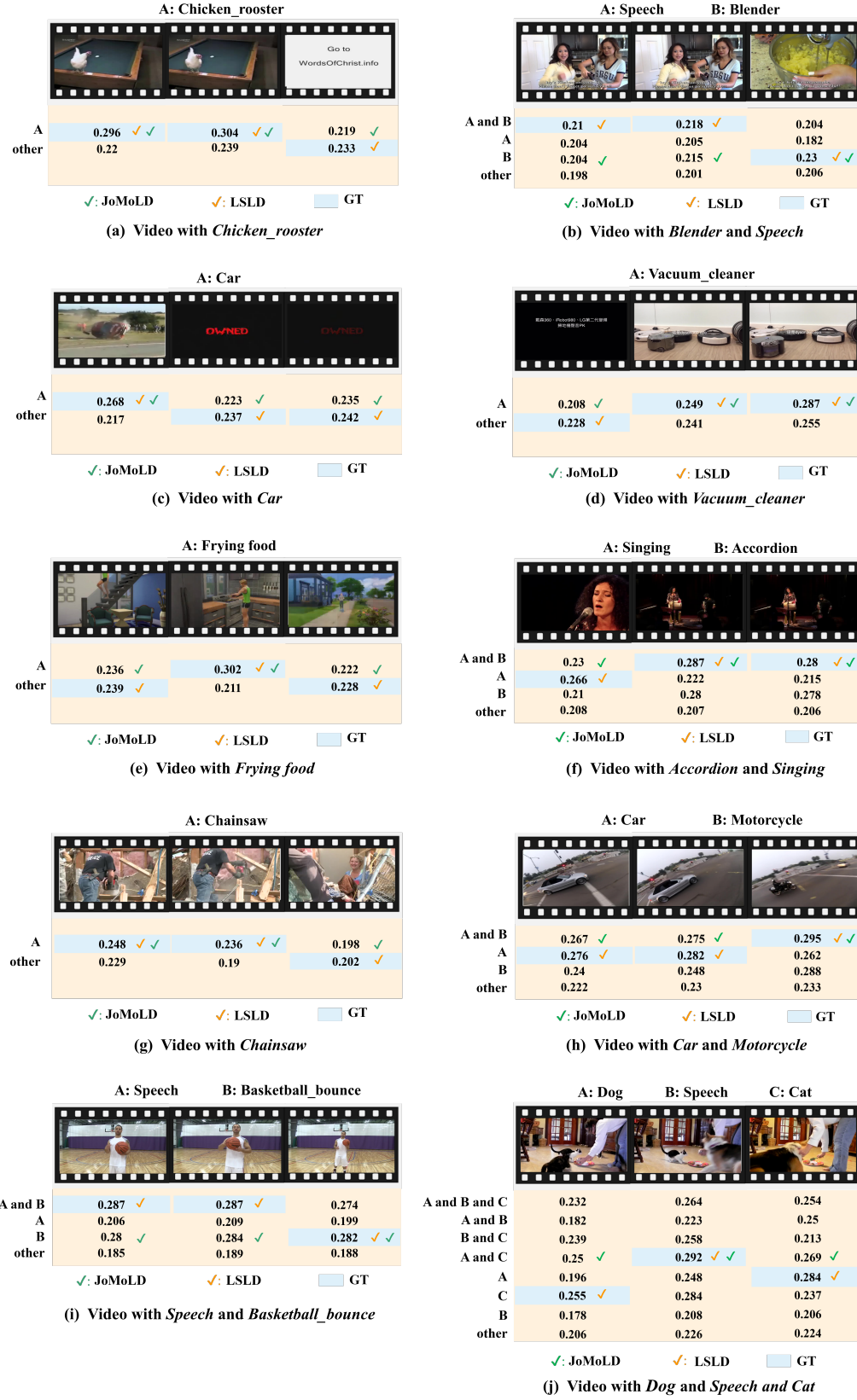


Figure 7: Visualization of more segment-level label denoising cases.

We provide more visualization cases for events like *Chicken rooster*, *Blender*, *Chainsaw* in Figure 7. LSLD successfully removes *Chicken rooster* in Figure 7 (a) when there is no chicken around. Similar cases are found in Figure 7 (c), (d), (e), (g). In addition, JoMoLD again fails to recognize *Speech* in some segments as illustrated in Figure 7 (b) and (i), which indicates that JoMoLD is more likely to recognize obvious events while our method is better at discriminating more classes. In Figure 7 (f), a person is *Singing* in the first segment with no one playing the *Accordion*, and LSLD removes *Accordion* from the segment label correctly, which indicates the effectiveness of our method. Also, in Figure 7 (h), though JoMoLD performs label denoising accurately on the video level, *Motorcycle* only appears in the last segment. On the other hand, LSLD provides a reasonable denoising of the labels at the segment level. Likewise, from Figure 6 (j), we can clearly see that *Dog* is not present in the first segment and *Cat* cannot be seen in the last one, but JoMoLD recognizes both *Cat* and *Dog* in all three of them. In conclusion, LSLD provides better label denoising capability than JoMoLD.